

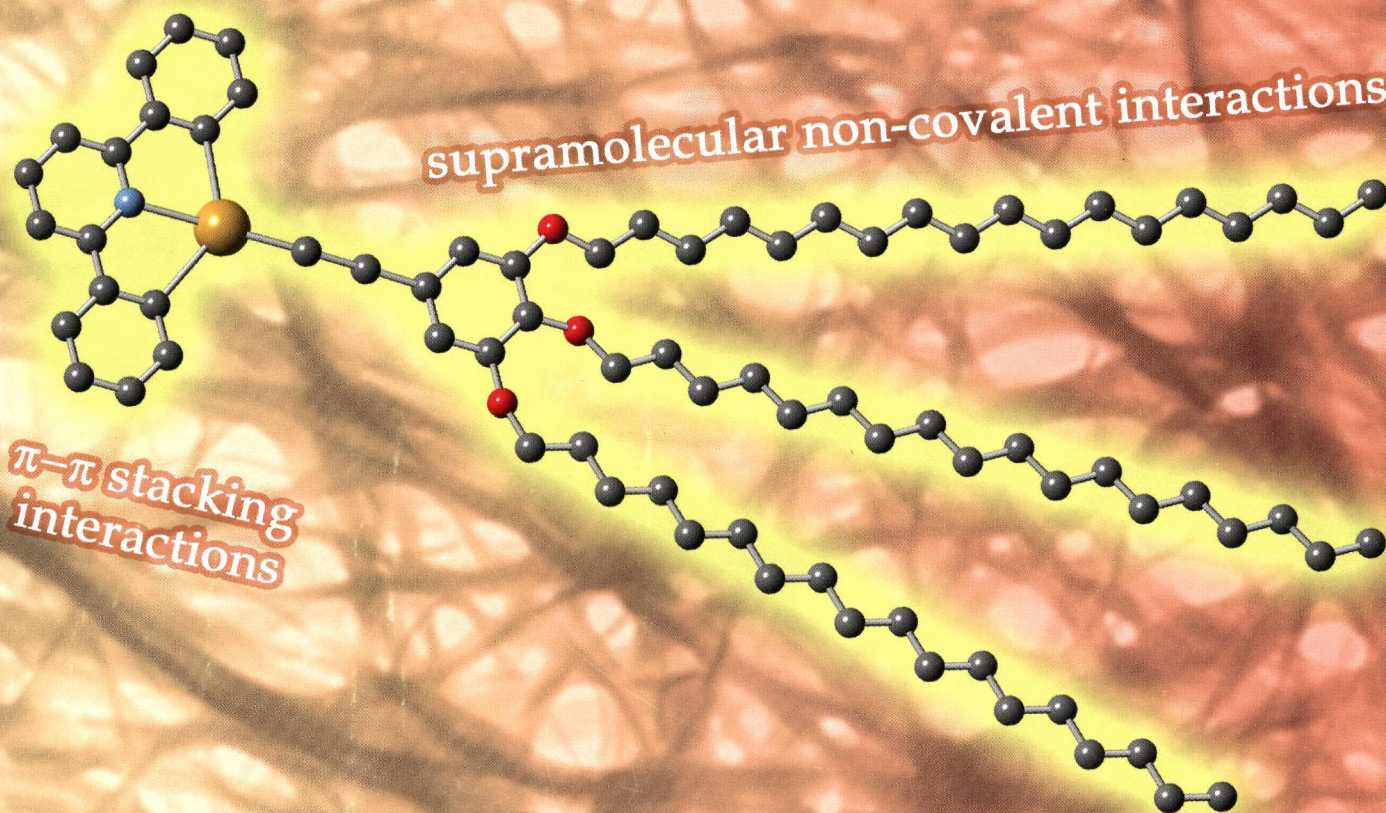
ПН
I-65

inorganic Chemistry

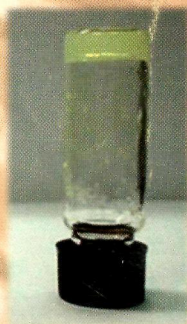
including bioinorganic chemistry

January 21, 2013
Volume 52, Number 2
pubs.acs.org/IC

Luminescent Au(III) Metallogels

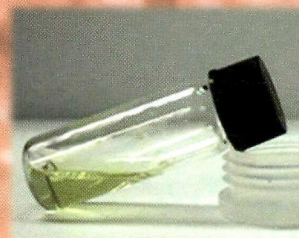


GEL



Cooling

Heating



SOL



ACS Publications
MOST TRUSTED. MOST CITED. MOST READ.

www.acs.org

ON THE COVER: A class of luminescent metallogels based on bis-cyclometalated alkynylgold(III) complexes has been developed. The gelation properties, which are driven by π - π stacking and supramolecular non-covalent interactions, have been investigated in detail by photophysical and electron microscopic studies. See V. K.-M. Au, N. Zhu, and V. W.-W. Yam, p 558.

Viewpoint

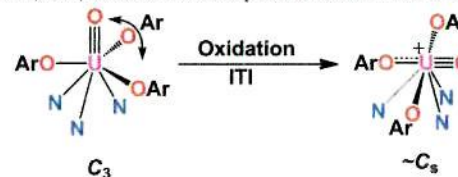
529

dx.doi.org/10.1021/ic302412j

Uranium–Ligand Multiple Bonding in Uranyl Analogues, $[L=U=L]^{n+}$, and the Inverse Trans Influence

Henry S. La Pierre and Karsten Meyer*

This Viewpoint Article reviews the theoretical, experimental, and synthetic work on the ITI in actinide complexes and contextualizes it within broader studies on the electronic structure of uranyl and its analogues. Furthermore, our recent work on the ITI in high-valent uranium(V/VI) oxo and imido complexes is described as a whole.



Communications

540

5

dx.doi.org/10.1021/ic3020404

Possible Superhardness of CrB₄

Arno Knappschneider, Christian Litterscheid, Dmytro Dzivenko, Joshua A. Kurzman, Ram Seshadri, Norbert Wagner, Johannes Beck, Ralf Riedel, and Barbara Albert*

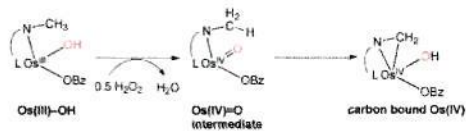
The Vickers hardness of chromium tetraboride is determined to be high, albeit not superhard, as suggested from theory. The previously proposed structure model is further refined to ensure the correctness of the description and to exclude the existence of two different orthorhombic phases with closely related space groups.



C–H Bond Activation of the Methyl Group of the Supporting Ligand in an Osmium(III) Complex upon Reaction with H₂O₂: Formation of an Organometallic Osmium(IV) Complex

Hideki Sugimoto,* Kenji Ashikari, and Shinobu Itoh*

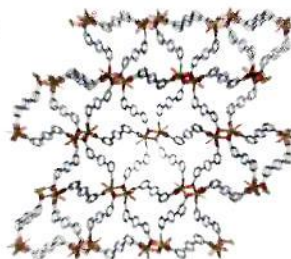
Oxidation of the hydroxoosmium(III) complex results in C–H bond activation of the methyl group of the supporting ligand. The obtained complex has a seven-coordinate osmium(IV) structure ligated with an additional Os^{IV}–CH₂ bond to the osmium(III) complex.



First Examples of Metal–Organic Frameworks with the Novel 3,3'-(1,2,4,5-Tetrazine-3,6-diyl)dibenzoic Spacer. Luminescence and Adsorption Properties

A. J. Calahorra, Antonio Peñas-Sanjuan, Manuel Melguizo, David Fairen-Jimenez, Guillermo Zaragoza, Belén Fernández, Alfonso Salinas-Castillo, and A. Rodríguez-Diéguez*

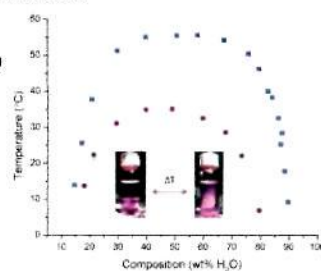
We report the synthesis of a novel ligand, 3,3'-(1,2,4,5-tetrazine-3,6-diyl)dibenzoic acid (1). In this fragment, we have introduced two carboxylate groups with the aim of using this ligand as a linker to construct three-dimensional metal–organic frameworks (MOFs). We have been successful in the formation of zinc (2) and lanthanum (3) MOFs. We include the luminescence, adsorption, and in vitro toxicity studies of these materials.



Switchable Phase Behavior of [HBet][Tf₂N]–H₂O upon Neodymium Loading: Implications for Lanthanide Separations

Daniel P. Fagnant Jr., George S. Goff,* Brian L. Scott, Wolfgang Runde, and Joan F. Brennecke*

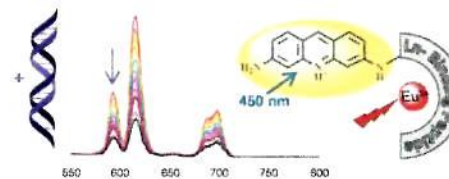
Temperature-dependent miscibility of the ionic liquid [HBet][Tf₂N] and H₂O before and after metal loading of neodymium(III). After neodymium(III) is introduced to the system, the upper critical solution temperature drops by over 20 °C. The temperature-dependent phase behavior can be utilized for the preconcentration of metal ions in the ionic liquid phase.



DNA Sensing by a Eu-Binding Peptide Containing a Proflavine Unit

Laetitia Ancel, Christelle Gateau, Colette Lebrun, and Pascale Delangle*

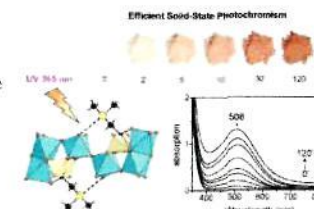
Synthesis of a lanthanide-binding peptide (LBP) for the detection of double-stranded DNA is presented. A proflavine moiety was introduced into a high affinity LBP involving two unnatural chelating amino acids in the Ln ion coordination. The Eu³⁺–LBP complex is demonstrated to bind to ct-DNA and to sensitize Eu luminescence. The DNA binding process is effectively detected via the Eu-centered luminescence thanks to the intimate coupling between the LBP scaffold and the DNA intercalating unit.



Sulfonium Polyoxometalates: A New Class of Solid-State Photochromic Hybrid Organic–Inorganic Materials

Khadija Hakouk, Olivier Oms, Anne Dolbecq, Hani El Moll, Jérôme Marrot, Michel Evain, Florian Molton, Carole Duboc, Philippe Deniard, Stéphane Jobic, Pierre Mialane,* and Rémi Dessapt*

We have shown that supramolecular hybrid organic–inorganic assemblies of polyoxometalates (POMs) and sulfonium cations show efficient solid-state photochromism under UV irradiation in ambient conditions, the color changes strongly depending on the nature of the POM units. The coloration kinetics have been determined by diffuse reflectance spectroscopy, and a new photochromism mechanism involving the photoreduction of the POM associated with electron transfers from the sulfonium cations toward the polyoxometalate core is proposed.



Articles

Luminescent Metallogels of Bis-Cyclometalated Alkynylgold(III) Complexes

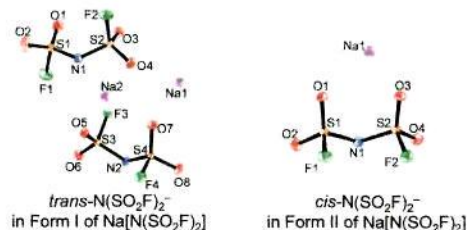
Vonika Ka-Man Au, Nianyong Zhu, and Vivian Wing-Wah Yam*

A series of luminescent bis-cyclometalated alkynylgold(III) complexes have been synthesized and characterized. Some of the complexes have been demonstrated to exhibit gelation properties driven by π – π stacking and hydrophobic–hydrophobic interactions. The gelation properties have been investigated in detail through variable-temperature UV–vis absorption and emission studies, and the morphology of the gels has also been characterized by scanning electron microscopy and transmission electron microscopy.



Polymorphism of Alkali Bis(fluorosulfonyl)amides [M(N(SO₂F)₂], M = Na, K, and Cs)
Kazuhiko Matsumoto,* Takaaki Oka, Toshiyuki Nohira, and Rika Hagiwara

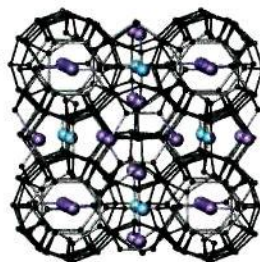
The polymorphic behavior of Na, K, and Cs salts of the bis(fluorosulfonyl)amide anion N(SO₂F)₂⁻ has been investigated by means of differential scanning calorimetry, single-crystal and powder X-ray diffraction, and Raman spectroscopy. It is found that polymorphism of these salts arises from the cis–trans conformational difference of N(SO₂F)₂⁻ as well as from differences in crystal packing.



Synthesis, Structure, and Transport Properties of Type-I Derived Clathrate Ge_{46-x}P_xSe_{8-y} (x = 15.4(1); y = 0–2.65) with Diverse Host–Guest Bonding

Maria A. Kirsanova, Takao Mori, Satofumi Maruyama, Maria Matveeva, Dmitry Batuk, Artem M. Abakumov, Andrei V. Gerasimenko, Andrei V. Olenev, Yuri Grin, and Andrei V. Shevelkov*

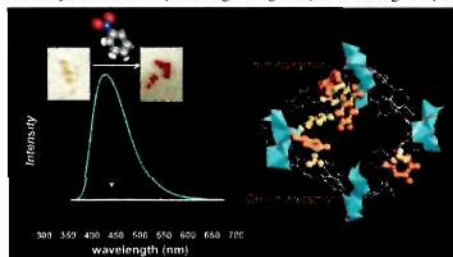
Selenium guest atoms show diverse host–guest bonding with the framework in a new clathrate Ge_{46-x}P_xSe_{8-y}, ranging from typical for clathrates weak interactions to a single covalent bond. The latter appears as a result of the framework transformation of the parent clathrate-I structure and relates the title phase to a scanty family of semiclathrates.



Luminescent Li-Based Metal–Organic Framework Tailored for the Selective Detection of Explosive Nitroaromatic Compounds: Direct Observation of Interaction Sites

Tae Kyung Kim, Jae Hwa Lee, Dohyun Moon,* and Hoi Ri Moon*

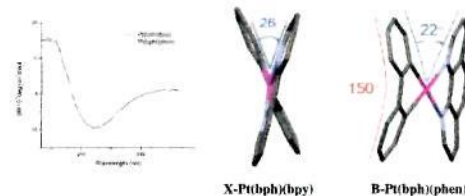
A luminescent lithium metal–organic framework constructed from Li⁺ and a well-designed organic ligand can selectively detect explosive nitroaromatic compounds by showing a dramatic color change with concurrent luminescence quenching in the solid state. The detection sites are proven directly through single-crystal-to-single-crystal transformations.



Electronic and Photophysical Properties of Platinum(II) Biphenyl Complexes Containing 2,2′-Bipyridine and 1,10-Phenanthroline Ligands

D. Paul Rillema,* Arvin J. Cruz, Curtis Moore, Khamis Siām, A. Jehan, Derek Base, T. Nguyen, and Wei Huang

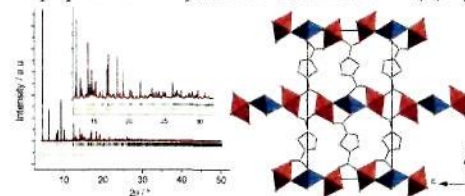
Pt(bph)(bpy) and Pt(bph)(phen) crystallized in the solid state in two configurations designated as X and B related to the orientation of the bph and diimine rings. Due to deviations from square planar geometry, the complexes exhibited chirality in solution. Both complexes underwent MLCT transitions near 440 nm and emission with nanosecond lifetimes at 77 K



Synthesis, Ab Initio X-ray Powder Diffraction Crystal Structure, and Magnetic Properties of Mn₃(OH)₂(C₆H₄O₄S)₂ Metal–Organic Framework

Romain Sibille,* Thomas Mazet, Erik Elkaïm, Bernard Malaman, and Michel François

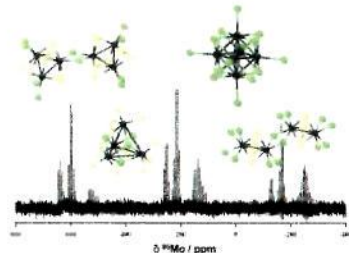
Mn₃(OH)₂(C₆H₄O₄S)₂, a new Metal–Organic Framework based on Mn(II) ions, hydroxides and 2,5-thiophenedicarboxylate ligands is presented. The crystal structure established from XRPD data shows unprecedented coordination of the dicarboxylate ligand and an original inorganic subnetwork whose structure is closely related to what is found in the M₂(OH)₂(1,4-benzenedicarboxylate) family. Magnetic and heat capacity measurements show antiferromagnetic ordering below T_N = 17.7 K. The magnetic properties are compared with those of other Mn(II) layered hybrid compounds.



617 **S** dx.doi.org/10.1021/ic301648s
⁹⁵Mo Solid-State Nuclear Magnetic Resonance Spectroscopy and Quantum Simulations: Synergetic Tools for the Study of Molybdenum Cluster Materials

Jérôme Cuny,* Stéphane Cordier, Christiane Perrin, Chris J. Pickard, Laurent Delevoeye,* Julien Trébosc, Zhehong Gan, Laurent Le Pollès, and Régis Gautier[‡]

The ability of ⁹⁵Mo solid-state nuclear magnetic resonance (SSNMR) spectroscopy to probe the atomic and electronic structures of inorganic molybdenum cluster materials has been demonstrated for the first time. A full interpretation of SSNMR spectra was enabled by the quantum-chemical calculations under periodic conditions of both chemical shielding and quadrupolar interaction parameters.

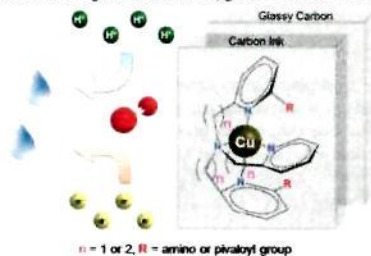


628 **S** dx.doi.org/10.1021/ic301656x

Ligand Effects on the Overpotential for Dioxygen Reduction by Tris(2-pyridylmethyl)amine Derivatives

Matthew A. Thorseth, Christopher S. Letko, Edmund C. M. Tse, Thomas B. Rauchfuss, and Andrew A. Gewirth*

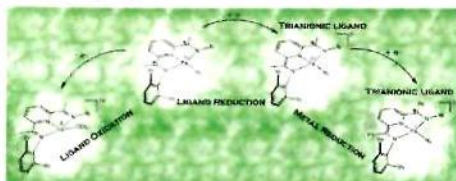
Coordination of Cu to ligands based on tris(2-pyridylmethyl)amine gives catalysts that are active for the oxygen reduction reaction, the efficacy of which depends on the ligand and the oxygen coordination environment.



635 **S** dx.doi.org/10.1021/ic301675t

Oxidation and Reduction of Bis(imino)pyridine Iron Dinitrogen Complexes: Evidence for Formation of a Chelate Trianion.
 Aaron M. Tondreau, S. Chantal E. Steiber, Carsten Milsmann, Emil Lobkovsky, Thomas Weyhermüller, Scott P. Sempronj, and Paul J. Chirik*

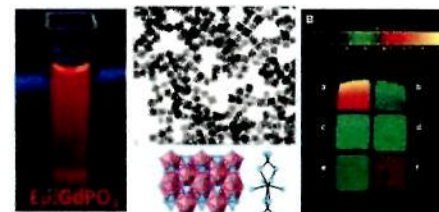
Oxidation and reduction of bis(imino)pyridine iron dinitrogen complexes have been explored and compounds that differ by four oxidation states have been prepared. The role of the redox-active bis(imino)pyridine has been established and rare examples of trianionic chelates have been identified.



647 **S** dx.doi.org/10.1021/ic3016996
Synthesis and Properties of Multifunctional Tetragonal Eu:GdPO₄ Nanocubes for Optical and Magnetic Resonance Imaging Applications

Sonia Rodriguez-Liviano, Ana I. Becerro, David Alcántara, Valeria Grazú, Jesus M. de la Fuente, and Manuel Ocaña*

Highly crystalline tetragonal Eu:GdPO₄ nanocubes (edge = 75 nm) have been synthesized which are nontoxic for cells and exhibit strong red luminescence and high transverse relaxivity (r₂) values. These properties make them suitable as biolabels for optical imaging and as negative contrast agent for magnetic resonance imaging.

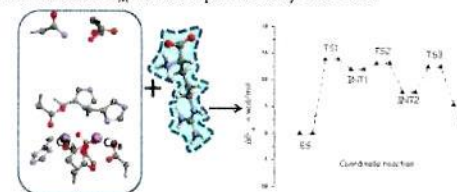


655 **S** dx.doi.org/10.1021/ic301703t

What Occurs by Replacing Mn²⁺ with Co²⁺ in Human Arginase I: First-Principles Computational Analysis

Tiziana Marino,* Nino Russo, and Marirosa Toscano

The catalytic mechanism of Co²⁺-arginase has been studied by using quantum-chemical calculations based on density functional theory methods. From the present theoretical investigation, it emerges that the cobalt enzyme works in way similar to the native one containing manganese. The binding energy of the ES complex in Co²⁺-arginase is higher than that in Mn²⁺-enzyme. This can account for the different K_M values experimentally observed.

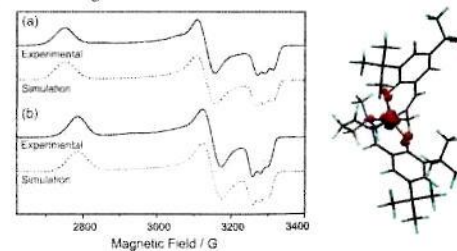


660 **S** dx.doi.org/10.1021/ic301731w

Five Coordinate M(II)-Diphenolate [M = Zn(II), Ni(II), and Cu(II)] Schiff Base Complexes Exhibiting Metal- and Ligand-Based Redox Chemistry

Mark Franks, Anastasia Gadzhieva, Laura Gandhi, David Murrell, Alexander J. Blake, E. Stephen Davies, William Lewis, Fabrizio Moro, Jonathan McMaster,* and Martin Schröder*

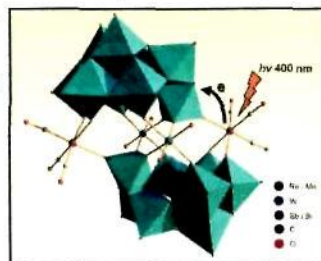
Incorporation of an additional single N-donor into the backbone of diphenolate N₂O₂-donor Schiff base ligands switches the redox chemistry of Ni^{II} complexes from ligand to metal-based SOMOs.



Synthesis, Structures, and Photochemistry of Tricarbonyl Metal Polyoxoanion Complexes, $[X_2W_{20}O_{70}\{M(CO)_3\}_2]^{12-}$ (X = Sb, Bi and M = Re, Mn)

Chongchao Zhao, Choon Sung Kambara, Ye Yang, Alexey L. Kaledin, Djameladdin G. Musaev, Tianquan Lian, and Craig L. Hill*

Four polytungstate-tricarbonyl metal derivatives, $[X_2W_{20}O_{70}\{M(CO)_3\}_2]^{12-}$ (X = Sb, Bi and M = Re, Mn), have been synthesized. These metal-donor-polyoxometalate-acceptor systems have been studied by single crystal X-ray diffraction, spectroscopic methods, femtosecond transient absorption spectroscopy, and computational modeling which collectively reveal charge-transfer processes from the Re/Mn centers on the structural periphery of the complex to the polyoxometalate ligands.



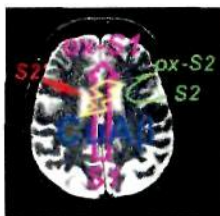
dx.doi.org/10.1021/ic301766b

Metal Binding of Flavonoids and Their Distinct Inhibition Mechanisms Toward the Oxidation Activity of Cu^{2+} - β -Amyloid: Not Just Serving as Suicide Antioxidants!

William Maung Tay, Giordano F. Z. da Silva, and Li-June Ming*

Two flavonoid families show distinctive antioxidation mechanism toward the oxidation reactions by $CuA\beta_{1-20}$: (a) the flavonols are competitive inhibitors and (b) the flavanols are substrates.

dx.doi.org/10.1021/ic301832p

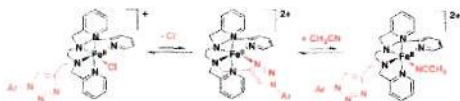


S1 = a Catecholamine neurotransmitter
S2 = a flavanol (suicide substrate)
S2 = a flavanol (competitive inhibitor)

Iron Coordination Chemistry with New Ligands Containing Triazole and Pyridine Moieties. Comparison of the Coordination Ability of the N-Donors

Nathalie Ségau, Jean-Noël Rebilly,* Katell Sénéchal-David, Régis Guillot, Laurianne Billon, Jean-Pierre Baltaze, Jonathan Farjon, Olivia Renaud, and Frédéric Banse*

Fe^{II} complexes based on tetradentate and pentadentate ligands (L_4 and L_5 , composed of two amines and two/three pyridines, respectively) functionalized with methoxyphenyl triazolyl groups have been obtained. Their characterization in acetonitrile allows to determine the structure of all of the species in equilibrium. For pentadentate ligands based on ethanediamine, ligand exchange is favored with a triazolyl group over a pyridyl one whereas no ligand exchange for $[L_3Fe^{II}\text{-triazolyl}]^{2+}$ with L_3 based on propanediamine.

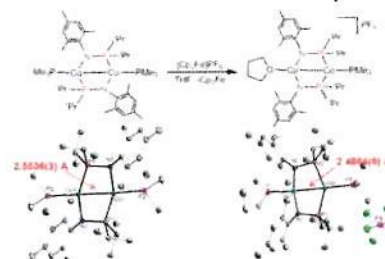


dx.doi.org/10.1021/ic301834x

Metal–Metal Bonding in Low-Coordinate Dicobalt Complexes Supported by Phosphinoamide Ligands

Ramyaa Mathialagan, Subramaniam Kuppaswamy, Alexandra T. De Denko, Mark W. Bezpalko, Bruce M. Foxman, and Christine M. Thomas*

Phosphinoamide-linked homobimetallic dicobalt complexes featuring Co centers in different coordination environments have been synthesized, and their multielectron redox chemistry has been investigated. Redox processes have been shown to promote ligand rearrangement in these low-coordinate metal–metal bonded species.

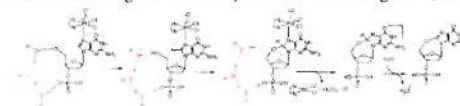


dx.doi.org/10.1021/ic3018375

Theoretical Investigation into the Mechanism of 3'-dGMP Oxidation by $[Pt^{IV}Cl_4(\text{dach})]$

Alireza Ariaifard,* Narges Mahdizadeh Ghohe, Kiana Khadem Abbasi, Allan J. Canty, and Brian F. Yates*

The detailed mechanism for oxidation of the guanine moiety of 3'-dGMP using $Pd^{IV}(\text{dach})Cl_4$ has been identified.



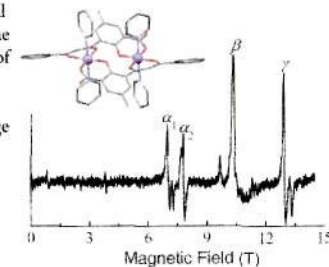
dx.doi.org/10.1021/ic3018425

Elucidating Magnetic Exchange and Anisotropy in Weakly Coupled Mn^{III} Dimers

Junjie Liu, J. Krzystek, Stephen Hill,* Leoní Barrios, and Guillem Aromí*

High-frequency EPR measurements have been performed on both a single-crystal and powder samples of a weakly coupled dinuclear $[Mn^{III}]_2$ molecular magnet. The single-crystal spectra provide a direct means of determining the axial anisotropy of the individual Mn^{III} ions and the exchange coupling between them. This work highlights the limitations of widely used protocols for analyzing magnetic and powder EPR data obtained for multinuclear molecular magnets in which exchange and anisotropy are comparable.

dx.doi.org/10.1021/ic301849f



PbMnIn₂S₅: Synthesis, Structure, and Properties

Peng Yu, Li-Ming Wu, and Ling Chen*

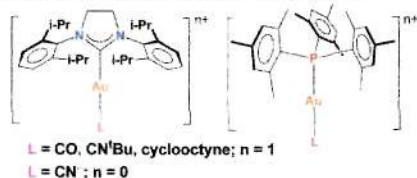
The first manganese member in Pb–M–In–Q system, PbMnIn₂S₅, has been discovered by high-temperature solid-state reaction. Mn and In atoms are disordered at two octahedral coordinated sites in the orthorhombic Sr₂I₂O₅ structure type lattice and antiferromagnetic interactions between the high-spin Mn²⁺ anions are observed.



End-On and Side-On π -Acid Ligand Adducts of Gold(I): Carbonyl, Cyanide, Isocyanide, and Cyclooctyne Gold(I) Complexes Supported by N-Heterocyclic Carbenes and Phosphines

Mehmet Ali Celik, Chandrakanta Dash, Venkata A. K. Adiraju, Animesh Das, Muhammed Yousufuddin, Gernot Frenking,* and H. V. Rasika Dias*

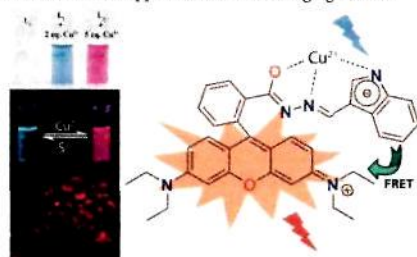
Synthesis, structures, and bonding of end-on bound carbonyl, cyanide, isocyanide, and side-on bound cyclooctyne adducts of gold(I) supported by the same N-heterocyclic carbene or phosphine are reported.



NIR- and FRET-Based Sensing of Cu²⁺ and S²⁻ in Physiological Conditions and in Live Cells

Chirantan Kar, Manab Deb Adhikari, Aiyagari Ramesh,* and Gopal Das*

This Article describes selective recognition of Cu²⁺ and S²⁻ in physiological conditions by NIR- and FRET-based techniques by indole functionalized rhodamine molecule and its application for cell-imaging studies.

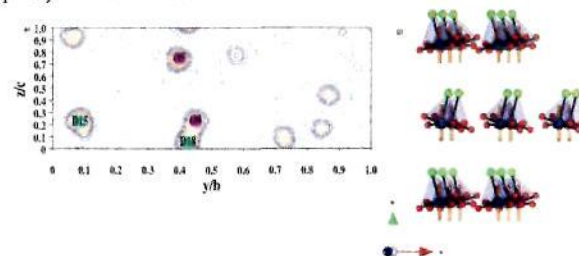


Magnetic Order Through Super-Superexchanges in the Polar Magnetoelectric Organic–Inorganic Hybrid

Cr[(D₃N-(CH₂)₂-PO₃)(Cl)(D₂O)]

Gwilherm Nénert,* Hyun-Joo Koo, Claire V. Colin, Elvira M. Bauer,* Carlo Bellitto, Clemens Ritter, Guido Righini, and Myung-Hwan Whangbo

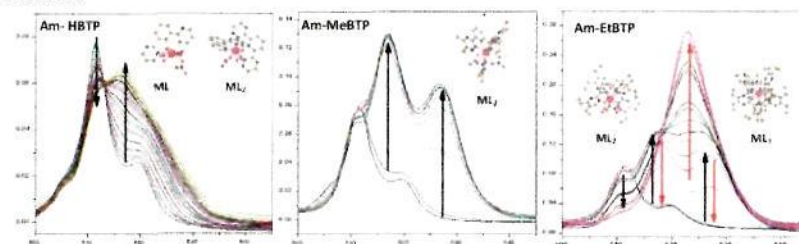
Partially deuterated Cr[(D₃N-(CH₂)₂-PO₃)(Cl)(D₂O)] has been studied by neutron powder diffraction and magnetization measurements down to 2 K. The precise crystal structure of the compound was determined. The strong magnetodielectric coupling reported and weak ferromagnetic component can be explained by the determined magnetic structure. The transition from paramagnetic to weakly ferromagnetic state results from super-superexchanges only and has been explained by theoretical analysis based on first-principles DFT calculations.



Trivalent Actinide and Lanthanide Complexation of 5,6-Dialkyl-2,6-bis(1,2,4-triazin-3-yl)pyridine (RBTP; R = H, Me, Et) Derivatives: A Combined Experimental and First-Principles Study

Arunasis Bhattacharyya,* Eunja Kim, Philippe F. Weck, Paul M. Forster, and Kenneth R. Czerwinski

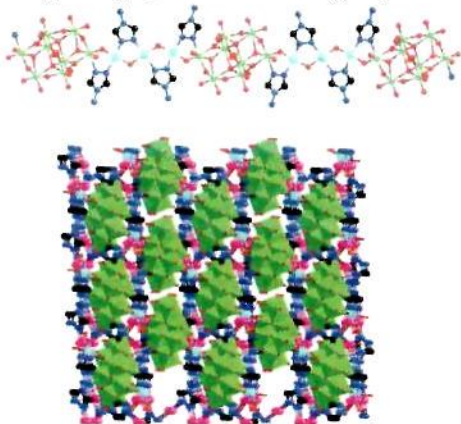
Americium(III) forms higher stoichiometric complexes with higher stability constants compared to the lanthanides of similar size, indicating the selectivity of these ligands for trivalent actinides. Their structures are depicted using density functional theory calculations.



Octamolybdate-Based Metal–Organic Framework with Unsaturated Coordinated Metal Center As Electrocatalyst for Generating Hydrogen from Water

Yun Gong, Tao Wu, Peng Gang Jiang, Jian Hua Lin,* and Yong Xi Yang

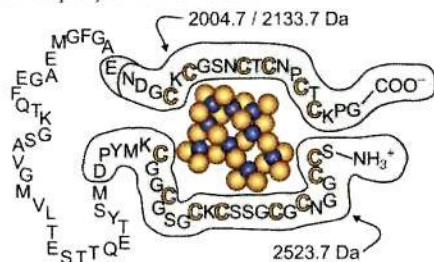
Two octamolybdate-based MOFs with unsaturated coordinated metal centers formulated as $\text{Cu}_3(\text{Mo}_8\text{O}_{26})(\text{H}_2\text{O})_2(\text{OH})_2(\text{L}1)_4$ ($\text{L}1 = 4H\text{-}4\text{-amino-}1,2,4\text{-triazole}$) (1) and $\text{Ag}_4(\text{Mo}_8\text{O}_{26})(\text{L}2)_{2.5}(\text{H}_2\text{O})$ ($\text{L}2 = 3,5\text{-dimethyl-}4\text{-amino-}4H\text{-}1,2,4\text{-triazole}$) (2) were synthesized and structurally characterized by single-crystal X-ray diffractions. The two complexes both exhibit electrocatalytic activities toward generating H_2 from water with lowered overpotentials and enhanced currents, and the Cu complex exhibits better electrocatalytic activity toward generating H_2 from water than the Ag complex.



Incorporation of Sulfide Ions into the Cadmium(II) Thiolate Cluster of *Cicer arietinum* Metallothionein2

Xiaoqiong Wan and Eva Freisinger*

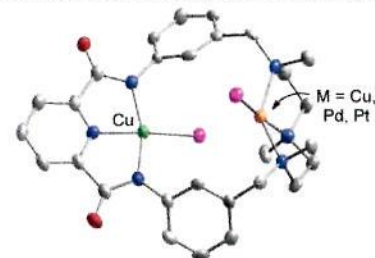
The Cd^{II} binding capacity of the plant metallothionein2 from *Cicer arietinum* (chickpea), *cic*-MT2, can be nearly doubled upon the incorporation of sulfide ions into the metal thiolate cluster. The resulting cluster arrangement featuring the stoichiometry $\text{Cd}_9\text{S-Cys}_{14}$ shows distinctively different features in the circular dichroism spectra and a significantly increased pH stability compared to the sulfide-free form. Sulfide incorporation into the metal thiolate clusters might be an economic and efficient strategy to increase the detoxification capacity of metallothionein.



Copper-, Palladium-, and Platinum-Containing Complexes of an Asymmetric Dinucleating Ligand

Mohammad Reza Halvagar, Benjamin Neisen, and William B. Tolman*

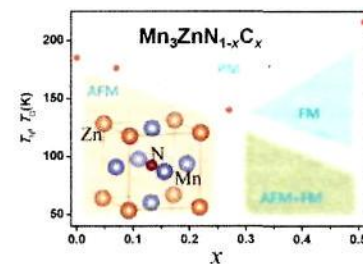
Exploration of the coordination chemistry of a ligand comprising neutral alkyltriamine and potentially dianionic dicarboxamido-pyridyl donor sets yielded monometallic, dicopper, and heterodinuclear Cu/Pd and Cu/Pt complexes.



Carbon-Induced Ferromagnetism in the Antiferromagnetic Metallic Host Material Mn_3ZnN

Ying Sun,* Yanfeng Guo, Yoshihiro Tsujimoto, Jijia Yang, Bin Shen, Wei Yi, Yoshitaka Matsushita, Cong Wang, Xia Wang, Jun Li, Clastin I. Sathish, and Kazunari Yamaura*

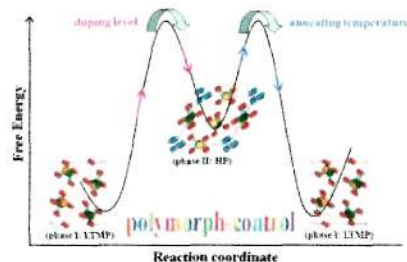
Carbon-for-nitrogen substitution (51 at% at most) was achieved in the antiferromagnetic metallic material Mn_3ZnN . The carbon-doped compounds were analyzed using synchrotron X-ray diffraction, and their electrical resistivities, specific heats, and degree of magnetizations were measured between temperatures of 2–400 K. The results demonstrate that the chemical tuning of the X site is as useful as that of the A and Mn sites for developing the properties of antiperovskite Mn_3AX materials for practical applications.



Is BiPO₄ a Better Luminescent Host? Case Study on Doping and Annealing Effects

Minglei Zhao, Liping Li, Jing Zheng, Liusai Yang, and Guangshe Li*

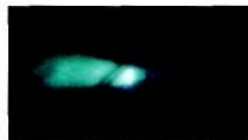
Here, we choose Eu-doped BiPO₄ as a model compound to study in which polymorphs were continuously transformed from monoclinic phase to hexagonal phase with increasing doping level. Such a phase transformation is totally altered upon annealing treatments. Interestingly, luminescence properties are highly sensitive to the corresponding crystal structures. The findings reported in this work are fundamentally important, which may provide significant references for designing new luminescent materials.



Probing the Chemical Nature of Dihydrogen Complexation to Transition Metals, a Gas Phase Case Study: H₂-CuF

Daniel J. Frohman, G. S. Grubbs II,* Zhenhong Yu, and Stewart E. Novick

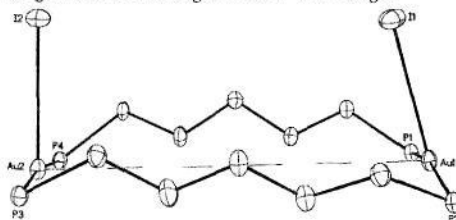
This work describes the observation of dihydrogen complexation to CuF using gas phase Fourier transform microwave (FTMW) spectroscopy. This is the first known FTMW observation of a dihydrogen complex to a metal containing molecule. The complex was synthesized using a combined laser ablation/supersonic expansion technique. All isotopologues are reported. A large increase in the copper electric quadrupole coupling constant from that of CuF combined with theoretical calculations indicates strong bonding consistent with transition metal σ bonding.



Crystallographic and Computational Studies of Luminescent, Binuclear Gold(I) Complexes, Au₂(Ph₂P(CH₂)_nPPh₂)₂ (n = 3–6)

Sang Ho Lim, Jennifer C. Schmitt, Jason Shearer,* Jianhua Jia, Marilyn M. Olmstead, James C. Fettinger, and Alan L. Balch*

Four luminescent, crystalline dimers of the type, Au₂(μ -PnP)₂, where PnP is PPh₂(CH₂)_nPPh₂ with n = 3, 4, 5, and 6 have been prepared and characterized by single-crystal X-ray diffraction and by ³¹P NMR and infrared spectroscopy. Computational and crystallographic studies indicate that the emission energies for the trigonal planar complexes are more strongly correlated with changes in the Au–I bond length rather than changes in the P–Au–P angle.



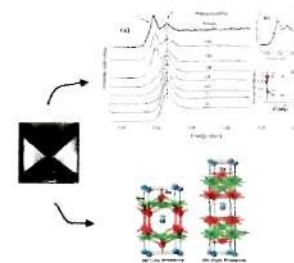
dx.doi.org/10.1021/ic301941k

dx.doi.org/10.1021/ic301954n

Pressure-Induced Valence and Structural Changes in YbMn₂Ge₂—Inelastic X-ray Spectroscopy and Theoretical Investigations

Ravhi S. Kumar,* A. Svane, G. Vaitheeswaran, Y. Zhang, V. Kanchana, M. Hofmann, S. J. Campbell, Yuming Xiao, P. Chow, Changfeng Chen, Yusheng Zhao, and Andrew L. Cornelius

High pressure resonant X-ray emission spectroscopy (RXES) and X-ray diffraction experiments (XRD) on YbMn₂Ge₂ show a pressure induced valence and structural change under compression. Yb becomes nearly trivalent around 30 GPa, and a tetragonal-monoclinic structural phase transition is observed above 35 GPa.

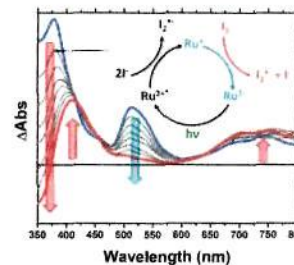


dx.doi.org/10.1021/ic302002u

Flash-Quench Studies on the One-Electron Reduction of Triiodide

Byron H. Farnum, William M. Ward, and Gerald J. Meyer*

The one-electron reduction of triiodide (I₃⁻) by a series of reduced ruthenium polypyridyl compounds was found to yield I₂^{•-} with an average second-order rate constant of $(5.0 \pm 0.6) \times 10^9 \text{ M}^{-1} \text{ s}^{-1}$ in acetonitrile at room temperature. The insensitivity of the rate constants to an 80 meV change in the driving force was unexpected. The relevance of these findings to solar energy conversion within dye-sensitized solar cells is discussed.

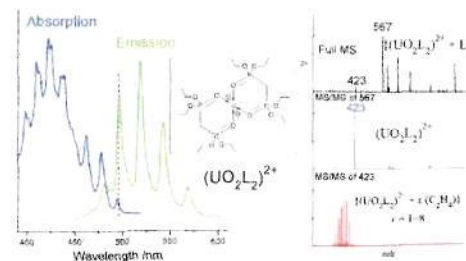


dx.doi.org/10.1021/ic302005e

A 2:1 Dicationic Complex of Tetraethyl Methylenebisphosphonate with Uranyl Ion in Acetonitrile and Ionic Liquids

Yupeng Liu, Taiwei Chu,* and Xiangyun Wang

A new 2:1 dicationic complex formed by tetraethyl methylenebisphosphonate (TEMBP) with uranyl ion in acetonitrile and two hydrophobic ionic liquids, [BMIm][NTf₂] and [N₄₁₁₁][NTf₂], has been identified as [UO₂(TEMBP)₂]²⁺ with combination of UV-vis absorption and luminescence emission spectroscopies and tandem ESI-ion trap mass spectrometry studies.



A Straight Forward Route for the Development of Metal–Organic Frameworks Functionalized with Aromatic –OH Groups: Synthesis, Characterization, and Gas (N_2 , Ar, H_2 , CO_2 , CH_4 , NH_3) Sorption Properties
Ioannis Spanopoulos, Pantelis Xydias, Christos D. Malliakas, and Pantelis N. Trikalitis*

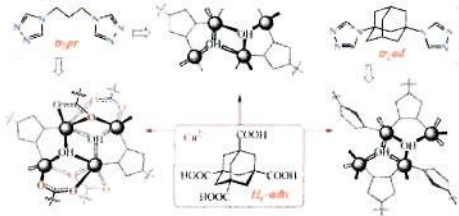
A straightforward synthetic route is presented for the development of MOFs functionalized with pendant, aromatic –OH groups.



Functionalized Adamantane Tectons Used in the Design of Mixed-Ligand Copper(II) 1,2,4-Triazolyl/Carboxylate Metal–Organic Frameworks

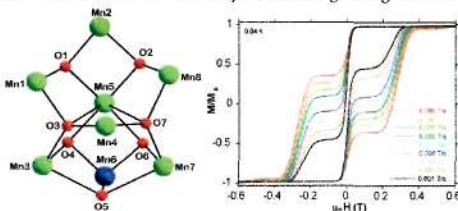
Ganna A. Senchuk, Andrey B. Lysenko,* Harald Krautscheid, Eduard B. Rusanov, Alexander N. Chernega, Karl W. Krämer, Shi-Xia Liu,* Silvio Decurtins, and Konstantin V. Domasevitch

The combination of bitopic 1,2,4-triazol-4-yl and rigid 1,3,5,7-adamantanetetracarboxylate ligands broadens the scope of the mixed-ligand approach in the design of copper(II) metal–organic frameworks built up from discrete tetranuclear dihydroxo clusters. The $\{Cu_4(OH)_2\}$ configurations are very sensitive to the ligand-type arrangements, which are mostly differentiated by coordination modes of –COO[−], tr heterocycle, as well as water molecules present in the cluster shell.



Comproportionation Reactions to Manganese(III/IV) Pivalate Clusters: A New Half-Integer Spin Single-Molecule Magnet
Shreya Mukherjee, Khalil A. Abboud, Wolfgang Wernsdorfer, and George Christou*

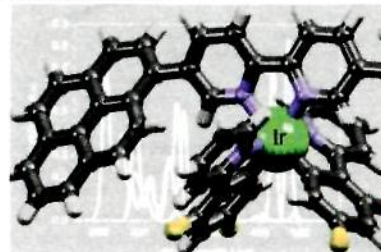
The comproportionation reaction between Mn^{II} and Mn^{VII} in the presence of pivalic acid has provided access to new mixed-valence clusters, $Mn^{III}_7Mn^{IV}_1$ (1) and $Mn^{III}_2Mn^{IV}_4$ (2), with unprecedented metal topologies, and a homovalent Mn^{III} , (3) cluster. Complex 1 has a rare $S = 15/2$ ground state and exhibits hysteresis in magnetization vs dc field sweeps at low temperatures, confirming it to be a new addition to the family of half-integer single-molecule magnets.



Ligand-Based Charge-Transfer Luminescence in Ionic Cyclometalated Iridium(III) Complexes Bearing a Pyrene-Functionalized Bipyridine Ligand: A Joint Theoretical and Experimental Study

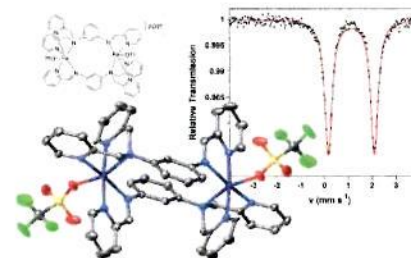
Edwin C. Constable, Markus Neuburger, Pirmin Rösel, Gabriel E. Schneider, Jennifer A. Zampese, Catherine E. Housecroft,* Filippo Monti, Nicola Armaroli,* Rubén D. Costa, and Enrique Ortí*

$[Ir(ppy)_2(py_r, bpy)] [PF_6]$ ($[1a][PF_6]$) and $[Ir(dfpp)_2(py_r, bpy)] [PF_6]$ ($[2a][PF_6]$), (Hppy = 2-phenylpyridine, Hdpppy = 2-(3,5-difluorophenyl)pyridine, and pyr₂bpy = 5,5'-bis(pyren-1-yl)-2,2'-bipyridine) are described and their electronic properties investigated. $[1a][PF_6]$ and $[2a][PF_6]$ exhibit intense absorptions around 400–500 nm arising from intramolecular charge-transfer transitions from pyrene to bipyridine domains. $[1a][PF_6]$ and $[2a][PF_6]$ exhibit luminescence bands centered above 650 nm, attributed to a charge-transfer triplet state located on the pyr₂bpy ligand. The luminescence (detected at room temperature and 77 K) shows that the appendage of luminophoric moieties to luminescent Ir-based centers may enhance the emission tuneability of this class of luminescent materials.



Syntheses and Electronic Structure of Bimetallic Complexes Containing a Flexible Redox-Active Bridging Ligand
Stacey Lindsay, Siu K. Lo, Oliver R. Maguire, Eckhard Bill, Michael R. Probert, Stephen Sproules, and Corinna R. Hess*

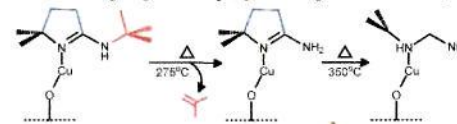
An asymmetric redox-active ligand provides a bridging scaffold for binuclear metal complexes. Spectroscopic, magnetic, and DFT computational studies provide insight regarding the electronic structures of and exchange interactions in these bimetallic complexes.



Copper Iminopyrrolidates: A Study of Thermal and Surface Chemistry

Jason P. Coyle, Peter J. Pallister, Agnieszka Kurek, Eric R. Sirianni, Glenn P. A. Yap, and Seán T. Barry*

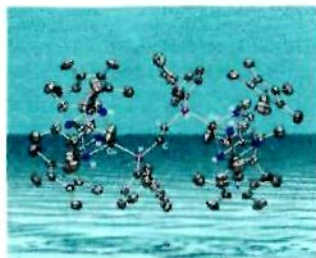
Copper(I) iminopyrrolidates show a high thermal stability because of the design of the ligand. Low temperature thermal decomposition pathways are thwarted through ligand design, permitting stable surface species up to 350°C.



Copper(I) and Silver(I) Complexes Supported by the Tridentate $[(Ti(\eta^5-C_5Me_5)(\mu-NH))_3(\mu_3-N)]$ Metalloligand

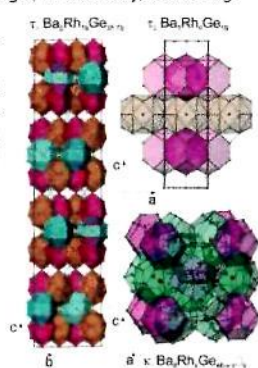
Avelino Martín, Noelia Martínez-Espada, Miguel Mena, Adrián Pérez-Redondo, and Carlos Yélagos*

Copper(I) and silver(I) complexes $[(CF_3SO_2O)M\{\mu_3-NH\}_3Ti_3(\eta^5-C_5Me_5)_3(\mu_3-N)]$ react with a variety of donor molecules L to give the ionic compounds $[(L)M\{\mu_3-NH\}_3Ti_3(\eta^5-C_5Me_5)_3(\mu_3-N)]^+ [O_3SCF_3]^-$ (L = NH₃, py, CNAr, CNtBu, PPh₃) whose cations contain $[MTi_3N_4]$ cube-type cores. The analogous treatment with bisphosphanes Ph₂P(CH₂)_nPPh₂ (n = 1, 2) gives 1:1 adducts $[(dppm)M\{\mu_3-NH\}_3Ti_3(\eta^5-C_5Me_5)_3(\mu_3-N)]^+ [O_3SCF_3]^-$ or 2:1 systems where a dppm or dppe ligand bridge two cube-type cations.

**Cage-Forming Compounds in the Ba–Rh–Ge System: From Thermoelectrics to Superconductivity**

M. Falmbigl, F. Kneidinger, M. Chen, A. Grytsiv, H. Michor, E. Royanian, E. Bauer, H. Effenberger, R. Podloucky, and P. Rogl*

Phase equilibria in the Ba–Rh–Ge system are characterized by three ternary cage compounds: τ_1 -BaRhGe₃ (BaNiSn₃-type) and two novel phases with unique structures, τ_2 -Ba₃Rh₄Ge₁₀ and τ_3 -Ba₃Rh₁₂Ge_{46–52}, besides κ_1 -Ba₃Rh₃Ge_{46–52} (x ≤ 1.2 and y ≥ 2.0). Density functional theory calculations for the enthalpies of formation and density of states for various compositions Ba₃Rh₃Ge_{46–52} (x = 0–6) demonstrate a strong stabilizing influence of Ge/Rh substitution. The physical properties have been investigated for κ_1 , τ_1 , τ_2 , and τ_3 , documenting a change from n-type thermoelectric (κ_1) to superconducting behavior (τ_2 ; T_c = 6.5 K).

**Synthesis, Properties, and Complex Crystal Structure of Th₂Se₅**

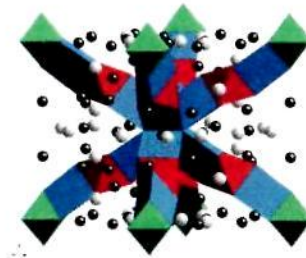
Brian J. Bellott, Christos D. Malliakas, Lukasz A. Koscielski, Mercouri G. Kanatzidis, and James A. Ibers*

The compound Th₂Se₅ has been synthesized and its structure determined by means of single-crystal X-ray diffraction methods.

**Li₁₁Nd₁₈Fe₄O_{39–δ} Revisited**

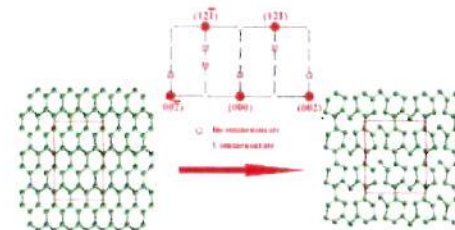
Peter D. Battle,* Sian E. Dutton, Fernande Grandjean, Gary J. Long, and Katsuyoshi Oh-ishi

The Mössbauer spectrum of Li₁₁Nd₁₈Fe₄O_{39–δ} has been reinterpreted. The relationship between Li₁₁Nd₁₈Fe₄O_{39–δ} and Li₁₈Li₈Fe₂O₃₉ is explored.

**Synthesis, Structural Characterization, and Physical Properties of the Early Rare-Earth Metal Digermanides REGe_{2–x} (x ≈ 1/4) [RE = La–Nd, Sm]. A Case Study of Commensurately and Incommensurately Modulated Structures**

Jiliang Zhang, Paul H. Tobash, William D. Pryz, Douglas J. Buttey, Namjung Hur, Joe D. Thompson, John L. Sarrao, and Svilen Bobev*

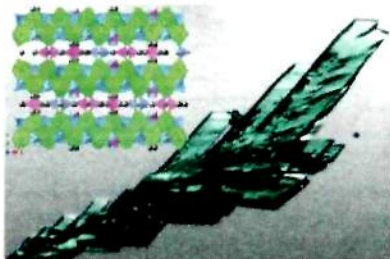
Vacancy ordered rare-earth metal germanides with general formula RE₂Ge- (RE = La–Nd, Sm) have been synthesized using the In-flux technique. Their structures have been established as variants of α-ThSi₂ structure type through long-range vacancy ordering. Electron diffraction reveals the coexistence of commensurate and incommensurate modulation in La and Ce compounds.



From Order to Disorder and Back Again: In Situ Hydrothermal Redox Reactions of Uranium Phosphites and Phosphates

Eric M. Villa, Connor J. Marr, Juan Diwu, Evgeny V. Alekseev,* Wulf Depmeier, and Thomas E. Albrecht-Schmitt*

Hydrothermal reactions of uranium with cesium carbonate and phosphorous acid yield several new structures, including two intermediate disordered 3D networks. These products span from uranyl phosphites, to disordered U^{IV} mixed phosphate–phosphite compounds, to two final stable products of uranium(IV) phosphate. The major influences for the products formed rely primarily on the starting pH, time, and the solubility of the crystalline products formed. The two transitional disordered compounds give insight into the complex reaction pathways within hydrothermal syntheses.



Novel Bis-C,N-Cyclometalated Iridium(III) Thiosemicarbazide Antitumor Complexes: Interactions with Human Serum Albumin and DNA, and Inhibition of Cathepsin B

José Ruiz,* Consuelo Vicente, Concepción de Haro, and Delia Bautista

Potent cytotoxic bis-C,N-cyclometalated iridium(III) thiosemicarbazide complexes for breast cancer cells (up to 5-fold more active than cisplatin in T47D) are described. Interactions with human serum albumin and DNA, and inhibition of cathepsin B has also been studied.



Phase Equilibria in the Mo–Fe–P System at 800 °C and Structure of Ternary Phosphide (Mo_{1-x}Fe_x)₃P (0.10 ≤ x ≤ 0.15)

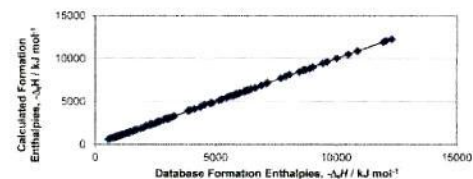
Anton O. Oliynyk, Yaroslava F. Lomnytska,* Mariya V. Dzevenko, Stanislav S. Stoyko, and Arthur Mar*

The Mo–Fe–P phase diagram reveals two ternary phases, including (Mo_{1-x}Fe_x)₃P (x = 0.10–0.15), which differs from the binary phase Mo₃P through a twisting of nets.



Single-Ion Values for Ionic Solids of Both Formation Enthalpies, Δ_fH(298)_{ion}, and Gibbs Formation Energies, Δ_fG(298)_{ion}, Leslie Glasser*

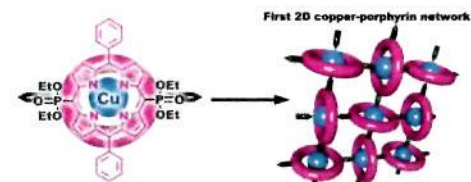
Single-ion formation enthalpies and Gibbs energies for a number of ionic solids, including a large group of silicates, have been established. Their sums provide excellent fits to the literature values. Values for ions not in the list may be evaluated by difference by reference to known thermodynamic values in related materials, but always with critical consideration of the results.



Unusual Formation of a Stable 2D Copper Porphyrin Network

Anna A. Sinelshchikova, Sergey E. Nefedov, Yulia Yu. Enakieva, Yulia G. Gorbunova,* Aslan Yu. Tsvadze, Karl M. Kadish, Ping Chen, Alla Bessmertnykh-Lemeune, Christine Stern, and Roger Guilard*

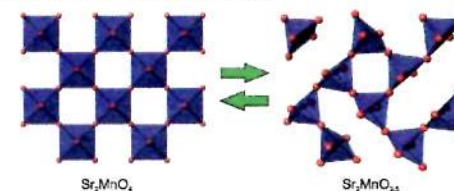
The first example of copper(II) meso-phosphorylated porphyrins that exists in the solid state in two polymorphic states—one consists of isolated molecules and another is the 2D coordination polymer—is described. The highly electron-withdrawing effect of the phosphoryl groups attached directly to the porphyrin macrocycle caused unprecedented formation of a stable 2D coordination network.



Reduction of Sr₂MnO₄ Investigated by High Temperature In Situ Neutron Powder Diffraction under Hydrogen Flow

Thibault Broux, Mona Bahout,* Olivier Hernandez, Florent Tonus, Serge Paofai, Thomas Hansen, and Colin Greaves*

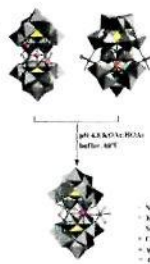
In situ neutron powder diffraction studies provide detailed structural information and kinetic data relating to the reversible transformation of tetragonal Sr₂MnO₄ into monoclinic Sr₂MnO_{3.5}.



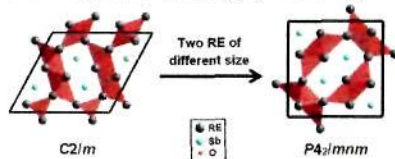

Di- and Tri-Cobalt Silicotungstates: Synthesis, Characterization, and Stability Studies

Guibo Zhu, Yurii V. Geletii, Jie Song, Chongchao Zhao, Elliot N. Glass, John Bacsa, and Craig L. Hill*

Di- and tricobalt silicotungstate complexes, $K_3Na_4H_4\{Na_3(\mu-OH)_2Co_2(\mu-OH)_4\}(Si_2W_{18}O_{66})\} \cdot 37H_2O$ (**1**) and $K_6Na_4[Na(H_2O)_3]_2\{Co(H_2O)_3\}_2\{Co(H_2O)_2\}(Si_2W_{18}O_{66})\} \cdot 22H_2O$ (**2**), have been synthesized and characterized. They both transform into $K_{11}[\{Co_2(H_2O)_8\}K(Si_2W_{18}O_{66})] \cdot 17H_2O$ (**3**) upon heating in potassium acetate buffer.

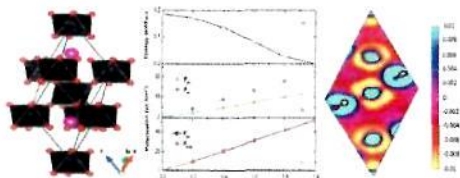
1025  dx.doi.org/10.1021/ic302292w**Synthesis, Crystal Structure, and Electronic Properties of the Tetragonal (RE^IRE^{II})₃SbO₃ Phases (RE^I = La, Ce; RE^{II} = Dy, Ho)**
Scott Forbes, Peng Wang, Jinlei Yao, Taras Kolodiaznyh, and Yuriy Mozharvskij*

The mixed (RE^IRE^{II})₃SbO₃ phases (RE^I = La, Ce; RE^{II} = Dy, Ho) were prepared via high-temperature reactions at 1550 °C. They adopt the $P4_2/mnm$ symmetry but have a structural framework similar to that of monoclinic RE₃SbO₃. The formation of the tetragonal (RE^IRE^{II})₃SbO₃ phases is driven by the ordering of the large and small RE atoms on different atomic sites. Electrical resistivity measurements indicate the presence of band gaps, which is supported by electronic structure calculations.

1032  dx.doi.org/10.1021/ic302298s**Structural, Electronic, and Ferroelectric Properties of Compressed CdPbO₃ Polymorphs**

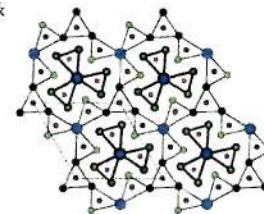
Yuanhui Xu, Xianfeng Hao, Cesare Franchini, and Faming Gao*

On the basis of density functional theory (DFT) and hybrid functional, we report a first-principles study for the structural, electronic, and ferroelectric properties of the two recently synthesized high-pressure polymorphs of CdPbO₃ with perovskite-type ($Pnma$) and LiNbO₃-type ($R3c$) structures. Besides providing the structural transformation and electronic results, we predict the realization of proper ferroelectric behavior in LiNbO₃-type CdPbO₃. On the basis of the Berry phase theory, the spontaneous electronic polarization is calculated as 52.3 $\mu C/cm^2$ along the $[111]$ direction. The origin of the ferroelectric behavior is discussed and explained in terms of the analysis of Born effective charges, potential-energy surfaces, charge density isosurfaces, and electric localization function.

**Rare-Earth Manganese Copper Pnictides RE₂Mn₃Cu₉Pn₇ (Pn = P, As): Quaternary Ordered Variants of the Zr₂Fe₁₂P₇-Type Structure**

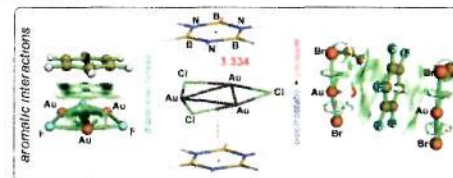
Stanislav S. Stoyko, Krishna K. Ramachandran, C. Scott Mullen, and Arthur Mar*

RE₂Mn₃Cu₉Pn₇ is built from Pn-centred trigonal prisms, generating a hexagonal framework such that Mn and Cu atoms are distributed in an ordered fashion.

1047  dx.doi.org/10.1021/ic302353t**Face-to-Face Stacks of Trinuclear Gold(I) Trihalides with Benzene, Hexafluorobenzene, and Borazine: Impact of Aromaticity on Stacking Interactions**

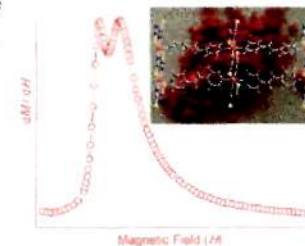
Athanasios C. Tzispis* and Alexandros V. Stalikas

The molecular and electronic structures, stabilities, bonding features, interaction energies, and magnetotropy of 1:1, 1:2, and 2:1 binary columnar stacks between $c-Au_3(\mu_2-X)_3$ clusters and benzene, hexafluorobenzene, or borazine are investigated employing electronic structure calculation methods.

1061  dx.doi.org/10.1021/ic302370n**Synthesis, Crystal Structure, and Magnetic Properties of the Coordination Polymer [Fe(NCS)₂(1,2-bis(4-pyridyl)-ethylene)]_n, Showing a Two Step Metamagnetic Transition**

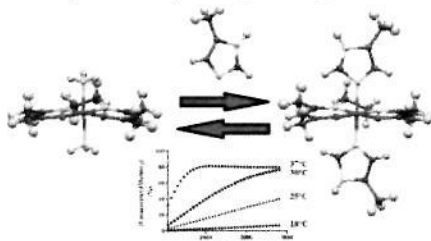
Susanne Wöhlert, Mario Wriedt, Tomasz Fic, Zbigniew Tomkowicz, Wolfgang Haase, and Christian Näther*

Reaction of iron(II) thiocyanate with an excess of *trans*-1,2-bis(4-pyridyl)-ethylene (bpe) in acetonitrile at room temperature leads to the formation of [Fe(NCS)₂(bpe)₂(bpe)] (**1**), which is isotypic to its Co(II) analogue. Using slightly different reaction conditions the literature known compound [Fe(NCS)₂(bpe)₂(H₂O)₂] (**2**) was obtained as a phase pure material. Simultaneous differential thermoanalysis and thermogravimetry prove that the hydrate **2** transforms into the anhydrate [Fe(NCS)₂(bpe)₂] (**3**), which decomposes upon further heating to [Fe(NCS)₂(bpe)]_n (**4**).



Axial Ligand Exchange of *N*-heterocyclic Cobalt(III) Schiff Base Complexes: Molecular Structure and NMR Solution Dynamics
Lisa M. Manus, Robert J. Holbrook, Tulay A. Atesin, Marie C. Heffern, Allison S. Harney, Amanda L. Eckermann, and Thomas J. Meade*

Co(III) Schiff base complex derivatives of bis(acetylacetonate)ethylenediimine [acacen] have been found to be potent enzyme and transcription factor inhibitors. Upon dissociation of its axial ligands, Co(III) irreversibly interacts with histidine residues of a target protein. The pD- and temperature-dependent axial ligand substitution dynamics of a series of *N*-heterocyclic [Co(acacen)(X)₂]⁺ complexes were characterized by NMR spectroscopy. Crystal structure analysis of the [Co(acacen)(X)₂]⁺ derivatives confirmed the trends in stability observed by NMR spectroscopy.



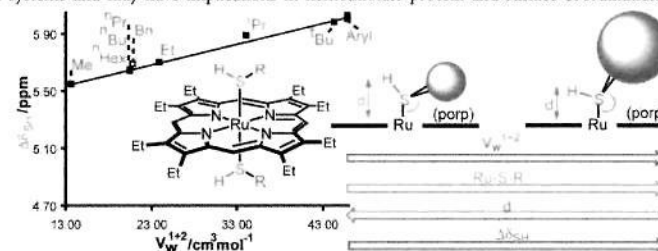
Probing the Nature of the Co(III) Ion in Corrins: Comparison of Reactions of Aquacyanocobyrinic Acid Heptamethyl Ester and Aquacyano-Stable Yellow Cobyrinic Acid Hexamethyl Ester with Neutral *N*-Donor Ligands
Susan M. Chemaly,* Louise Kendall, Monika Nowakowska, Dale Pon, Christopher B. Perry, and Helder M. Marques*

Equilibrium constants ($\log K$) for substitution of coordinated H₂O in aquacyanocobyrinic acid heptamethyl ester (aquacyanocobester, ACCbs) and aquacyano-stable yellow-cobyrinic acid hexamethyl ester (aquacyano-stable yellow cobester, ACSYCBs), in which oxidation of the C5 carbon of the corrin interrupts the normal delocalized system of corrins, by neutral *N*-donor ligands (ammonia, ethanolamine, 2-methoxyethylamine, *N*-methylimidazole, and 4-methylpyridine) have been determined spectrophotometrically as a function of temperature.



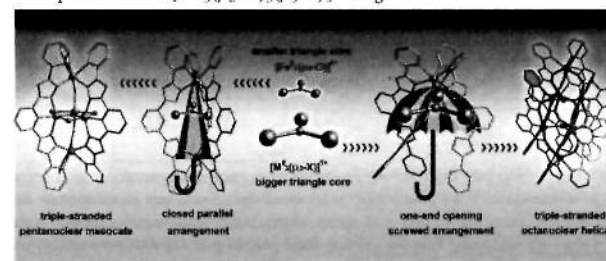
Molecular Recognition Using Ruthenium(II) Porphyrin Thiol Complexes as Probes
Júlio S. Rebouças and Brian R. James*

Upfield ¹H NMR shifts for the SH proton within 106 Ru(porp)(RSH)₂ species (porp = porphyrin dianion; R = alkyl or aryl) are analyzed in terms of nonbonding electronic and steric factors of substituents within the porp and thiol fragments, and an empirical model is formulated to explain the data quantitatively. The findings are relevant to molecular recognition within metalloporphyrin systems and may have implications in hemethiolate protein and surface coordination chemistry.



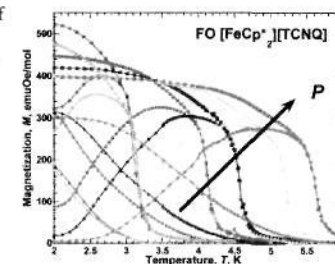
Self-Assembly of Pentanuclear Mesocate versus Octanuclear Helicate: Size Effect of the [M^{II}₃(μ₃-O/X)]⁺ Triangle Core
Xin Bao, Wei Liu, Jun-Liang Liu, Silvia Gómez-Coca, Eliseo Ruiz,* and Ming-Liang Tong*

The size effect of the [M^{II}₃(μ₃-O/X)]⁺ triangle core on the assembly of 2,6-bis[5-(2-pyridinyl)-1*H*-triazol-3-yl]pyridine ligands and metal ions is investigated: a smaller triangle core prefers a pentanuclear mesocate, while a bigger triangle core stabilizes an octanuclear helicate. Density functional theory calculations show that main exchange interactions are those with antiferromagnetic character present in the [M^{II}₃(μ₂-Cl)₃(μ₃-O)] triangles.



Pressure-Dependent Enhanced *T*_c and Magnetic Behavior of the Metamagnetic and Ferromagnetic Polymorphs of [Fe^{II}Cp*₂]⁺[TCNQ]⁻ (Cp* = Pentamethylcyclopentadienide; TCNQ = 7,7,8,8-Tetracyano-*p*-quinodimethane)
Jack G. DaSilva and Joel S. Miller*

The magnetic behaviors of the metamagnetic and ferromagnetic polymorphs of [Fe^{II}Cp*₂]⁺[TCNQ]⁻ (Cp* = pentamethylcyclopentadienide; TCNQ = 7,7,8,8-tetracyano-*p*-quinodimethane) were studied as a function of hydrostatic pressure. Both polymorphs exhibit a reversible enhancement of magnetic properties with increasing pressure.



2,2,2-Tris(pyrazolyl)ethoxide (Ep^{OX}) Ruthenium(II) Complexes, (Ep^{OX})RuCl(L)(L'): Synthesis, Structure, and Reactivity

Brandon Quillian, Evan E. Joslin, T. Brent Gunnoe,* Michal Sabat, and William H. Myers

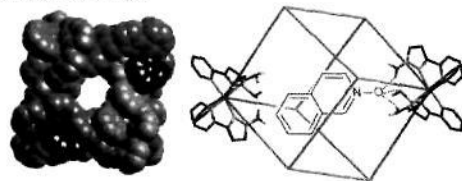
2,2,2-Tris(pyrazolyl)ethanol (Ep^{OX}) has been utilized as a facially κ^3 -N₃N₃O-coordinating ligand on a series of Ru(II) complexes. The image shows that the PPh₃ ligands can be substituted with other ligands to provide several new Ru(II) compounds of the type (Ep^{OX})RuCl(L)(L'). The compounds convert into cationic tris(pyrazolyl)methane Ru(II) complexes upon heating in chloroform.



Shape-, Size-, and Functional Group-Selective Binding of Small Organic Guests in a Paramagnetic Coordination Cage

Simon Turega, Martina Whitehead, Benjamin R. Hall, Anthony J. H. M. Meijer, Christopher A. Hunter,* and Michael D. Ward*

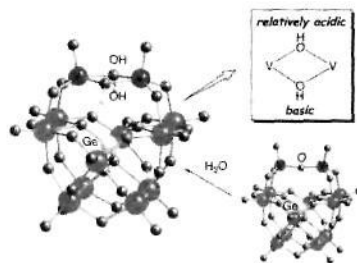
A cubic coordination cage acts in MeCN as a host for neutral organic guests which contain an H-bond-accepting group that interacts with the internal surface of the cage. The different thermodynamic contributions to guest recognition and the kinetics of both guest binding and reorganization inside the cavity have been analyzed in detail by ¹H NMR spectroscopy, which is facilitated by the paramagnetism of the host cage.



Effects of Isolobal Heteroatoms in Divanadium-Substituted γ -Keggin-type Polyoxometalates on (OV)₂(μ -OH)₂ Diamond and (OV)₂(μ -O) Core Structures and the Transformation

Kazuhiro Uehara, Tatsuya Taketsugu, Kazuhiro Yonehara, and Noritaka Mizuno*

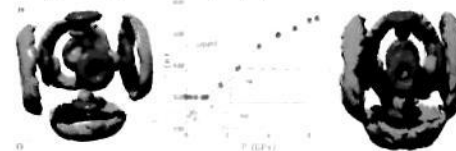
Heterolytic dissociation of water with the (μ -oxo)divanadium core in (TBA)₄[γ -GeV₂W₁₀O₃₈(μ -O)]²⁻ to form the bis(μ -hydroxo)divanadium core is confirmed by a crystal-to-crystal transformation. The dissociation proceeds through coordination of water on coordinatively unsaturated vanadium center via the lowest unoccupied molecular orbital (LUMO), followed by proton transfer to the bridging oxo moiety. The order is different from that in (TBA)₄[γ -SiV₂W₁₀O₃₈(μ -O)]²⁻ because of the lower energy level of the highest occupied molecular orbital (HOMO) of ²G₆ (lower nucleophilicity toward a water proton) than that of ²S₀.



Hydration Properties of the Zn²⁺ Ion in Water at High Pressure

Valentina Migliorati,* Giordano Mancini, Simone Tatoli, Andrea Zitolo, Adriano Filipponi, Simone De Panfilis, Andrea Di Cicco, and Paola D'Angelo*

The hydration properties of the Zn²⁺ ion under high pressure conditions have been investigated using a combined approach based on extended X-ray absorption fine structure (EXAFS) spectroscopy and Molecular Dynamics (MD) simulations. The Zn²⁺ first shell retains an octahedral geometry also at very high pressure while the first hydration shell is contracted.



Lifetime Heterogeneity of DNA-Bound dppz Complexes Originates from Distinct Intercalation Geometries Determined by Complex-Complex Interactions

Johanna Andersson, Louise H. Forander, Maria Abrahamsson, Eimer Tuite, Pär Nordell, and Per Lincoln*

A global fit to isothermal titration calorimetry and excited-state lifetime binding isotherms for [Ru(L)₂dppz]²⁺ with AT-DNA suggest that a symmetrical and an asymmetrical intercalation mode give rise to the short and the long emission lifetime, respectively. The relative abundance of the two binding modes is determined by a combination of cooperative and anticooperative interactions that are sensitive to both the chirality of the complex and the structure of the ancillary ligands L.

